Journal of Power Sources 229 (2013) 272–276

Contents lists available at SciVerse ScienceDirect

Journal of Power Sources

journal homepage: www.elsevier.com/locate/jpowsour

Short communication

Temperature dependent local structure of $LiCoO_2$ nanoparticles determined by Co K-edge X-ray absorption fine structure

L. Maugeri [a], L. Simonelli [b], A. Iadecola [a,c], B. Joseph [a], M. Okubo [d], I. Honma [e], H. Wadati [f], T. Mizokawa [g,h], N.L. Saini [a,*]

[a] Dipartimento di Fisica, Università di Roma "La Sapienza", P. le Aldo Moro 2, 00185 Roma, Italy
[b] European Synchrotron Radiation Facility, 6 RUE Jules Horowitz, BP 220, 38043 Grenoble Cedex 9, France
[c] Elettra, Sincrotrone Trieste, Strada Statale 14, Km 163.5, Basovizza, Trieste, Italy
[d] National Institute of Advanced Industrial Science and Technology (AIST), Umezono 1-1-1, Tsukuba, Ibaraki 305-8578, Japan
[e] Multidisciplinary Research for Advanced Materials, Tohoku University, Sendai, Miyagi 980-8577, Japan
[f] Department of Applied Physics and Quantum-Phase Electronics Center (QPEC), University of Tokyo, Hongo, Tokyo 113-8656, Japan
[g] Department of Physics, University of Tokyo, 5-1-5 Kashiwanoha, Kashiwa, Chiba 277-8561, Japan
[h] Department of Complexity Science and Engineering, University of Tokyo, 5-1-5 Kashiwanoha, Kashiwa, Chiba 277-8561, Japan

HIGHLIGHTS

- Temperature dependent local disorder in $LiCoO_2$ bulk and nanoparticles is studied.
- The nanostructuring is found to have direct influence on the bondlength characteristics, in addition to the random disorder.
- The Co–O bond strength is substantially changed in nanoparticles in comparison with the bulk.

ARTICLE INFO

Article history:
Received 11 August 2012
Received in revised form
6 November 2012
Accepted 29 November 2012
Available online 12 December 2012

Keywords:
$LiCoO_2$ nanoparticles
Local disorder
Lithium-ion batteries
X-ray absorption spectroscopy

ABSTRACT

Temperature dependent Co K-edge extended X-ray absorption fine structure is used to investigate local disorder in $LiCoO_2$ nanoparticles. We find that the nanostructuring has direct influence on the bondlength characteristics. The results reveal a substantial decrease in the force constant of Co–O bonds (the Co–O bonds becoming more flexible), while that for the Co–Co bonds showing hardly any change (or increases slightly) in $LiCoO_2$ nanoparticles with respect to the bulk. Therefore, both random disorder and Co–O bondlength flexibility should be the factors to limit the battery characteristics of the $LiCoO_2$ nanoparticles.

1. Introduction

The structure of cathode materials greatly influences the efficiency of Li ion batteries including the reversibility of the Li ions diffusion [1–4]. Among others, Li_xCoO_2 is a well known cathode material for the rechargeable Li ion batteries. Most of the Li_xCoO_2 cathodes in use are bulk materials in which the lifetime is the main concern because during the charging a compact crystal structure (bulk) sustains bond breaking, having direct consequences on the reversibility of ion migration in the cathode [1–3]. Nanoparticles can be used to overcome this problem due to strain compensation characteristics led by increased surface area [5–8]. This should be beneficial for the battery life and reversible delithiation/lithiation of the cathode material during the charging/discharging.

Indeed, battery characteristics are found to be highly influenced with variation of particle size in $LiCoO_2$ nanoparticles cathode [8]. Moreover, there appears a critical particle size below which the use of nanoparticles is not beneficial with the characteristics degrading with further reduction of the size [8]. Since structural disorder in nanoparticles is one of the main concerns, we have recently addressed this problem and studied local structure of $LiCoO_2$ nanoparticles by X-ray absorption spectroscopy [9]. Being an

*Corresponding author. Tel.: +39 0649914387; fax: +39 064957697.
E-mail address: Naurang.Saini@roma1.infn.it (N.L. Saini).

0378-7753/$ – see front matter © 2013 Elsevier B.V. All rights reserved.
http://dx.doi.org/10.1016/j.jpowsour.2012.11.127

atomic site-specific experimental probe [10], X-ray absorption spectroscopy has been widely used to study local structural aspects in a variety of systems, including the materials in rechargeable Li-batteries [11–16]. From the study of size dependence of $LiCoO_2$ nanoparticles [9], we have found that the nanoparticles are characterized by an atomic disorder similar to that occurring during the charging (delithiation) process. In this work, we have studied the local structure of $LiCoO_2$ nanoparticles by temperature dependent extended X-ray absorption fine structure (EXAFS). Temperature dependent measurements are needed to separate the static disorder from the thermal disorder. In addition, temperature dependent EXAFS permits to extract direct information on the bondlength characteristics, i.e. bond strength determined by the force constants. From the temperature dependent Co K-edge EXAFS measurements we have found that the Co–O bond strength in the $LiCoO_2$ nanoparticles is significantly reduced while the Co–Co bondlengths hardly sustaining any change (or getting slightly stiffer) with respect to the bulk material. Present study reveals that the static disorder and the atomic displacements in the CoO_6 octahedra are the two limiting factors for a reversible diffusion of Li ion in the $LiCoO_2$ nanoparticles.

2. Experimental details

X-ray absorption measurements were performed at the beamline BM23 in the European Synchrotron Radiation Facility (ESRF), Grenoble on well characterized powder samples of $LiCoO_2$ nanoparticles prepared by hydrothermal reaction method [8]. The estimated uncertainties in the average particle size were about ±3 nm. The details of synthesis and characterization are reported in detail elsewhere [8]. The synchrotron radiation emitted by a bending magnet source at 6 GeV ESRF storage ring was monochromatized by a double crystal Si(311) monochromator. The absorption measurements at the Co K-edge were made in transmission mode. The samples were mounted in a continuous flow He cryostat and the temperature was controlled and monitored within an accuracy of ±1 K. Several spectral scans were acquired at each temperature to ensure the spectral reproducibility. Standard procedure based on the cubic spline fit to the pre-edge subtracted absorption spectrum was used to extract the EXAFS signal [10] to determine local structural parameters.

3. Results and discussion

Fig. 1 shows Fourier transform (FT) magnitudes of the EXAFS oscillations extracted from Co K-edge X-ray absorption spectra measured at several temperatures on $LiCoO_2$ bulk and nanoparticles of different size. The FT provides information on the partial atomic distribution around the Co atoms in the $LiCoO_2$ system. The FT shows single scattering contributions from the nearest neighbour O atoms at a distance ~1.92 Å, and the next nearest neighbours Co atoms at a distance ~2.81 Å. The contribution of Co–Li distance (~2.97 Å) is hardly seen due to negligible scattering factor of lithium in comparison with Co. The peaks at longer distances are due to multiple scattering contributions. The effect of temperature is apparent, appearing different for the bulk and the nanoparticles. There is hardly any change in the peak positions with temperature and the particle size, however, the peak amplitude is seen to be suppressed for the nanoparticles, consistent with larger disorder [9].

To quantify the differences in the local disorder we have modelled the EXAFS oscillation due to single scattering. In the single-scattering approximation, the EXAFS amplitude is described by the following general equation [10]:

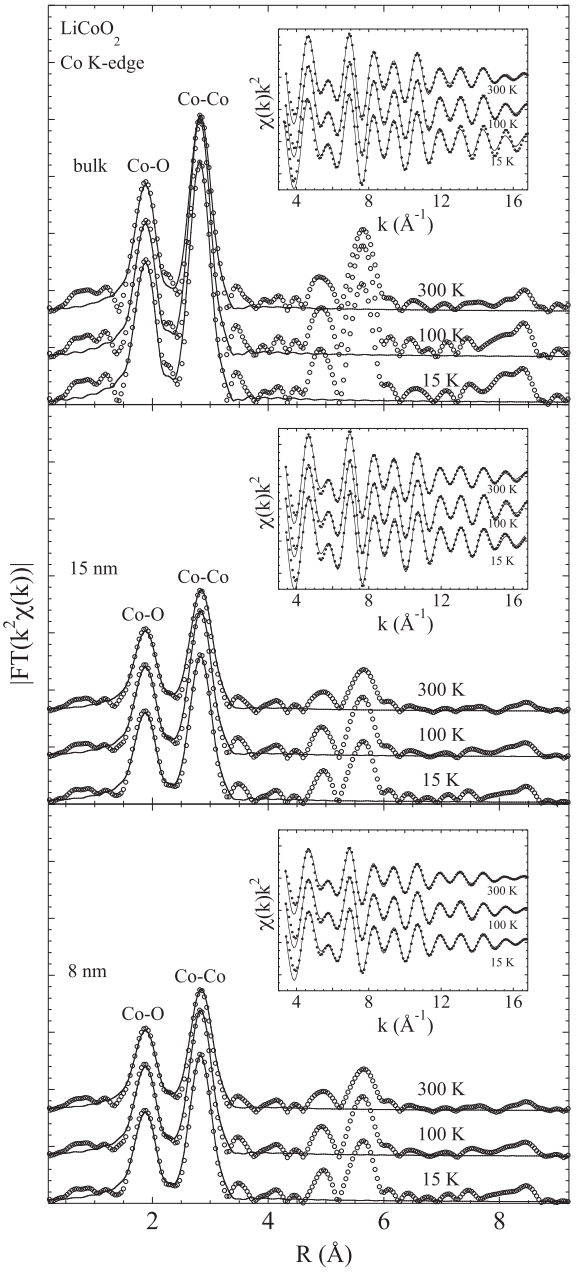

Fig. 1. Fourier transform magnitudes of the Co K-edge EXAFS (weighted by k^2) measured on $LiCoO_2$ bulk (upper) and nanoparticles of different size (middle and lower) at several temperatures. A Gaussian window is used to perform the FT using k-range of 3-17Å^{-1}. Model fits to the FT are also shown (solid curves). Model fits to the experimental filtered EXAFS in the k-space are also shown (insets).

$$\chi(k) = \sum_i \frac{N_i S_0^2}{kR_i^2} f_i(k,R_i) e^{-\frac{2R_i}{\lambda}} e^{-2k^2\sigma_i^2} \sin[2kR_i + \delta_i(k)] \quad (1)$$

where N_i is the number of neighbouring atoms at a distance R_i, $f_i(k,R_i)$ is the backscattering amplitude, λ is the photoelectron mean free path, δ_i is the phase shift, and σ_i^2 is the correlated Debye–Waller factor (DWF) measuring the mean square relative displacements (MSRDs) of the photoabsorber–backscatter pairs. The S_0^2 is the so-called passive electrons reduction factor, i.e., EXAFS amplitude reduction factor due to many-body effects related with the losses occuring during the photoelectron propagation in the material (excitations as plasmons, electron–hole pairs, etc.) and the

intrinsic losses due to shake-up and shake-off excitations created by the core-hole in the absorption process. While it is difficult to quantify these many-body effects, chemical transferability is best procedure for the estimation of the S_0^2 [10,17].

We have used EXCURVE 9.275 code (with calculated backscattering amplitudes and phase shift functions) for the EXAFS model fits [18] to the single scattering contributions due to Co–O and Co–Co bonds, well separated from any multiple scattering contributions. The N_i was fixed to the average values known from diffraction studies [19]. The E_0 and S_0^2 were fixed after a number of fit trials on five different scans at a fixed temperature on the bulk sample. The best fit values for the S_0^2 were found to be 0.9 for the Co–O shell and 1.0 for the Co–Co shell. These values are consistent with the available EXAFS literature on oxides revealing S_0^2 to be between 0.7 and 0.9 for metal-oxygen and 0.8–1.0 for the metal–metal pairs, depending on the metal and the structural configurations [17,20,21]. We did not see any appreciable change in the N_i with decreasing particle size (except for the 8 nm sample in which the N_i was ~5.6 instead of the diffraction value of $N_i = 6$). The fact that no appreciable change in the N_i was observed unlike some earlier studies on nanoparticles [22], a possible agglomeration of smaller size nanoparticles is not ruled out. Only the distances R_i and the corresponding σ_i^2, were the fit parameters in the least squares modelling. The number of independent data points, $(N_{\text{ind}} \sim 2\Delta k\Delta R)/\pi$ [10] were about 18 ($\Delta k = 14$ Å^{-1} and $\Delta R = 2.4$ Å), in the four parameters fits (i.e., Co–O and Co–Co distances and the corresponding σ_i^2). The uncertainties were determined by creating correlation maps with appropriate contour level established by modelling different scans. Any contribution from Co–Li distance (~2.97 Å) was ignored due to negligible scattering factor of lithium compared to the Co. Possible anharmonic effects due to large atomic vibrations were checked including higher order cumulants [23], however, the difference with the harmonic case was negligible, and hence not considered in the final fits. The model fits in the *k*-space EXAFS are included in the insets of Fig. 1. The real space model fits are also included in the Figure. Here, the goodness of fit is determined by the statistical *R*-factor defined as;

$$R = \sum_i^N \frac{1}{s_i}\left(\left|\chi_i^{\text{exp}}(k) - \chi_i^{\text{th}}(k)\right|\right) * 100\% \quad (2)$$

where N is the number of data points, s_i the standard deviation for each data point i and $\chi_i^{\text{exp}}(k)$ and $\chi_i^{\text{th}}(k)$ the experimental and theoretical EXAFS, respectively. The *R* factors for the filtered EXAFS fits were found to be between 12 and 13 for all the samples, indicating very good fits (see, e.g. the insets of Fig. 1).

Fig. 2 shows local bondlengths determined by Co K-edge EXAFS analysis as a function of temperature for $LiCoO_2$ bulk and the nanoparticles. The particle size for the bulk sample is estimated [8] to be 200 nm. Both Co–O and Co–Co distances tend to increase with decreasing nanoparticle size, consistent with earlier studies [8,9]. There is a small temperature effect due to the thermal expansion, appearing different for different particle size, albeit the differences are within the experimental uncertainties.

Fig. 3 shows the correlated Debye Waller factors (σ^2), i.e., the MSRDs of the Co–O and the Co–Co pairs as a function of temperature for the $LiCoO_2$ bulk and nanoparticles. The temperature dependence of σ^2 for Co–Co bonds looks nearly the same, however, the one for the Co–O bonds is apparently different between the bulk sample and the nanoparticles. It should be recalled that the EXAFS Debye Waller factors (distance–distance correlation function, i.e., the distance broadening) is sum of temperature

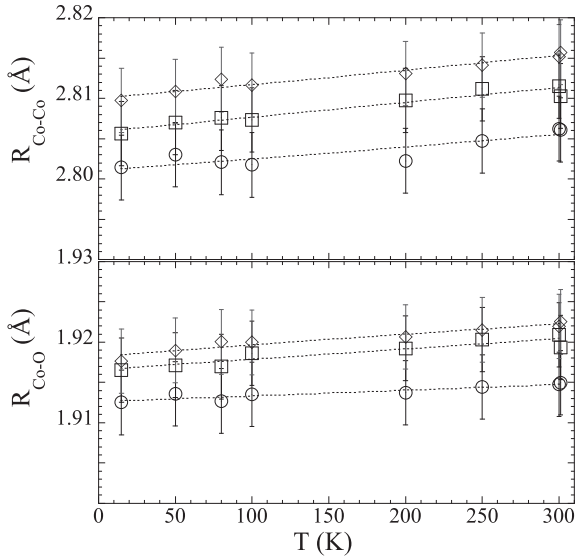

Fig. 2. The near neighbour Co–O and Co–Co distances in the $LiCoO_2$ bulk (circles) and nanoparticles (diamonds and squares represent 8 nm and 15 nm samples respectively) as a function of temperature. The bondlengths are consistent with the average distances measured by diffraction [8].

independent (σ_0^2) and temperature dependent terms, i.e. $\sigma^2 = \sigma_0^2 + \sigma^2(T)$. Generally a correlated Einstein (or Debye) model is used to describe the $\sigma^2(T)$ measured by EXAFS experiments [10]. While a well-defined frequency of local optical modes is used in the Einstein model, one has to integrate over the vibrational density of

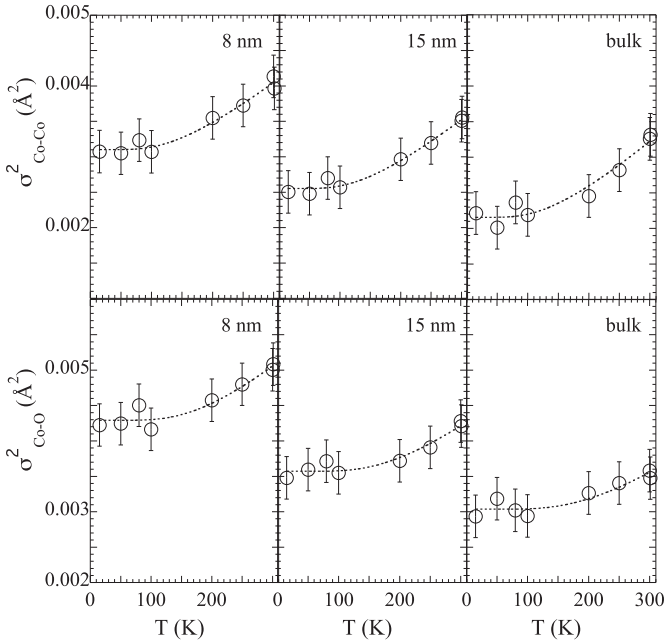

Fig. 3. Temperature dependence of Co–O (lower) and Co–Co (upper) MSRDs (symbols) for the $LiCoO_2$ bulk (right) and nanoparticles of 15 nm (middle) and 8 nm (left). The solid lines represent the correlated Einstein model fits. The Einstein-temperatures (θ_E) for the Co–O bonds are 720 ± 45 K, 678 ± 36 K and 645 ± 30 K respectively for the bulk, 15 nm and 8 nm samples. The σ_0^2 for the Co–O bonds are ~0.0004, ~0.0008 and ~0.0014 respectively for the bulk, 15 nm and 8 nm samples, indicating a large static disorder in the nanoparticles. On the other hand, the θ_E for the Co–Co bonds are 443 ± 18 K, 458 ± 20 K and 462 ± 21 K for the bulk, 15 nm and 8 nm samples respectively. The σ_0^2 for the Co–Co bonds are ~0.0003, ~0.0008 and ~0.0014 respectively for the bulk, 15 nm and 8 nm samples, again consistent with larger static disorder in the nanoparticles.

states (VDOS) (including acoustic modes) in the Debye model. However, in the harmonic and single scattering approximation the simplest model to describe the temperature dependence of $\sigma^2(T)$ is the correlated Einstein model, and the difference between the Einstein and Debye models is generally smaller than the experimental and theoretical uncertainties in the low temperature regime [24,25]. Here, the $\sigma^2(T)$ is well described by the correlated Einstein model [10,24,25], an appropriate approximation considering the temperature range. The Einstein equation to describe the $\sigma^2(T)$ is:

$$\sigma^2(T) = \frac{\hbar^2}{2\mu k_B \theta_E} \coth \frac{\theta_E}{2T} \quad (3)$$

The Einstein temperature (θ_E, i.e., the Einstein frequency $\omega_E = k_B\theta_E/\hbar$) for the Co–O pairs tend to decrease in the nanoparticles with respect to the bulk, indicating a decreased local force constant of this bond ($k = \mu\omega_E^2$, where k is the effective force constant and μ is reduced mass of the Co–O pair). Indeed, the estimated θ_E for the Co–O bonds in the bulk, 15 nm and 8 nm were 720 ± 45 K, 678 ± 36 K and 645 ± 30 K respectively. The corresponding force constants are ~25.1 eV Å^{-2}, ~22.3 eV Å^{-2} and ~20.1 eV Å^{-2} for the three samples. Therefore, it appears that the local Co–O bondlengths are getting relatively flexible with nanostructuring in $LiCoO_2$. Also, the temperature independent part of the correlated Debye Waller factors for the nanoparticles (σ_0^2 = 0.0008 Å^2 and 0.0014 Å^2 respectively for the 15 nm and 8 nm samples) is larger than the bulk sample (σ_0^2 = 0.0004 Å^2), consistent with much larger static disorder in the nanoparticles. Here, it is worth mentioning that the static disorder in the bulk represent mainly the configuration disorder, however, with decreasing the particle size from bulk to the nanoparticles, the static disorder is expected to have significant contribution of surface/interface disorder.

On the other hand, the θ_E for the Co–Co bondlength hardly shows any change with the particle size. The θ_E (force constants) for the Co–Co bonds in the bulk, 15 nm and 8 nm were found to be 443 ± 18 K (~9.5 eV Å^{-2}), 458 ± 20 K (~10.1 eV Å^{-2}) and 462 ± 21 K (~10.3 eV Å^{-2}) respectively, showing a negligible change (or a tendency of increase). However, there is a clear increase of σ_0^2 also for the Co–Co bonds with nano-structuring, found to be 0.0003 Å^2, 0.0008 Å^2 and 0.0014 Å^2 respectively for the bulk, 15 nm and 8 nm samples, mere indication of increasing static disorder with decreasing particle size. Therefore, in general the nanostructuring induces static disorder including the surface/interface disorder. In addition, it appears that the local Co–O bondlengths are relatively relaxed, while the Co–Co bonds hardly show any change (or becomes a little stiffer) in the nanoparticles of $LiCoO_2$, suggesting large atomic displacements in the CoO_6 octahedral configuration.

Earlier we have studied [9] X-ray absorption near edge structure (XANES) spectra of the $LiCoO_2$ nanoparticles, probing higher order atomic distribution function. From the XANES analysis it was found that the nanoparticles behave as if $LiCoO_2$ bulk is being delithiated, i.e. there is an apparent increase in the Co valency. However, it is different from Li deficient bulk samples of $LiCoO_2$ that show [26] substantial change in the Co–O distance, which decreases with delithiation. On the other hand, in-situ studies have revealed increase of c-axis lattice constant during Li extraction [27]. In the present case, the Co–O distance increases with decreasing particles size (opposite to the Co–O distance change due to partial delithiation as argued above). This indicates that the origin of the disorder may not be a simple Li deficiency, but the change of octahedral configuration. Indeed, the present study has clearly underlined the fact that, in addition to the static disorder, nanostructuring has direct and substantial influence on the bondlength characteristics. In particular, the Co–O suffers a large change in the bondlength strength, a mere indication of large atomic displacements within the CoO_6 octahedra, and hence the electronic configuration. In fact, the delithiation can be viewed as increase of the average valence of Co (consistent with the XANES analysis [9]), i.e., a part of the Co^{3+} is getting transformed in Co^{4+}, which is a Jahn–Teller ion with d^5 configuration. The Jahn–Teller distortions of the CoO_6 octahedra have natural consequences on the force constant of Co–O bonds, getting more flexible in the nanoparticles. On the other hand, the $LiCoO_2$ nanoparticles seems to be characterized by Co^{3+} ions with coexisting Jahn–Teller distorted octahedra (Co^{4+} ions). Increased Co–O bondlengths and reduced bond strength with decreasing particles size should be due to the Jahn–Teller distorted octahedra. Therefore, in addition to the static disorder, octahedral atomic displacements are important in the nano-structuring.

In summary, we have studied temperature dependent local structure of the $LiCoO_2$ bulk and nanoparticles by Co K-edges X-ray absorption spectroscopy. The EXAFS data provide clear evidence of local disorder in the nanoparticles, increasing with the decreasing particle size. In addition to the increasing static disorder, the Co–O bond strength shows a substantial decrease with reducing particle size while the Co–Co distances hardly suffer any change in their strength (or tending to get stiffer). In conclusion, the study of the local structure of $LiCoO_2$ nanoparticles underlines the key role of local atomic displacements in the CoO_6 octahedra and disorder, being limiting factors for the diffusion and the reversibility of the Li^+ intercalation when $LiCoO_2$ nanoparticles are used as cathodes for batteries.

Acknowledgements

The authors wishes to thank ESRF staff for the help and support during the experimental runs. This research is partially supported by the Japan Society for the Promotion of Science (JSPS) through the 'FIRST Program' initiated by the Council for Science and Technology Policy.

References

[1] J.B. Goodenough, Y. Kim, Chem. Mater. 22 (2010) 587.
[2] P. He, H. Yu, D. Li, H. Zhou, J. Mater. Chem. 22 (2012) 3680.
[3] J.-M. Tarascon, M. Armand, Nature 414 (2001) 359 (and references therein).
[4] J. Choi, A. Manthiram, Phys. Rev. B 74 (2006) 205114.
[5] P. Poizot, S. Laruelle, S. Grugeon, L. Dupont, J.-M. Tarascon, Nature 407 (2000) 496.
[6] A.R. Armstrong, G. Armstrong, J.R. Canales Garcia, P.G. Bruce, Adv. Mater. 17 (2005) 862.
[7] A.S. Arico, P. Bruce, J.-M. Tarascon, W.V. Schalkwijk, Nat. Mater. 4 (2005) 366.
[8] M. Okubo, E. Hosono, J. Kim, M. Enomoto, N. Kojima, T. Kudo, H. Zhou, I. Honma, J. Am. Chem. Soc. 129 (2007) 7444;
M. Okubo, J. Kim, T. Kudo, H. Zhou, I. Honma, J. Phys. Chem. C 113 (2009) 15337.
[9] L. Maugeri, A. Iadecola, B. Joseph, L. Simonelli, L. Olivi, M. Okubo, I. Honma, H. Wadati, T. Mizokawa, N.L. Saini, J. Phys. Condens. Matter 24 (2012) 335305.
[10] R. Prins, D.C. Koningsberger (Eds.), X-ray Absorption: Principles, Applications, Techniques of EXAFS, SEXAFS, XANES, Wiley, New York, 1988.
[11] J. McBreen, J. Solid State Electrochem. 13 (2009) 1051.
[12] A.V. Chadwick, S.L.P. Savin, R. Alcantara, D.F. Lisbona, P. Lavela, G.F. Ortiz, J.L. Tirado, ChemPhysChem 7 (2006) 1086.
[13] W.-S. Yoon, K.-K. Lee, K.-B. Kim, J. Electrochem. Soc. 149 (2002) A146.
[14] P. Shearing, Y. Wu, S.J. Harris, N. Brandon, Electrochem. Soc. Interface 20 (2011) 43.
[15] Y.W. Tsai, B.J. Hwang, G. Ceder, H.S. Sheu, D.G. Liu, J.F. Lee, Chem. Mater. 17 (2005) 3191.
[16] M. Balasubramanian, X. Sun, X.Q. Yang, J. McBreen, J. Power Sources 92 (2001) 1; M. Balasubramanian, X. Sun, X.Q. Yang, J. McBreen, J. Electrochem. Soc. 147 (2000) 2903.
[17] G.G. Li, F. Bridges, C.H. Booth, Phys. Rev. B 52 (1995) 6332.
[18] S.J. Gurman, J. Synch. Rad. 2 (1995) 56.
[19] J. Akimoto, Y. Gotoh, Y. Oosawa, J. Solid State Chem. 141 (1998) 298.

[20] A. Bianconi, N.L. Saini, Struct. Bonding 114 (2005) 287.
[21] M. Filippi, B. Kundys, S. Agrestini, W. Prellier, H. Oyanagi, N.L. Saini, J. Appl. Phys. 106 (2009) 104116.
[22] A.I. Frenkel, C.W. Hills, R.G. Nuzzo, J. Phys. Chem. B 105 (2001) 12689.
[23] P. Fornasini, F. Monti, A. Sanson, J. Synchrotron Radiat. 8 (2001) 1214.
[24] E. Sevillano, H. Meuth, J.J. Rehr, Phys. Rev. B20 (1979) 4908.
[25] See, e.g. a review by J.J. Rehr, R.C. Albers, Rev. Mod. Phys. 72 (2000) 621.
[26] J.M. Rosolen, P. Ballirano, M. Berrettoni, F. Decker, M. Gregorkiewitz, Ionics 3 (1997) 345.
[27] G.G. Amatucci, J.-M. Tarascon, L.C. Klein, Solid State Ionics 83 (1996) 167.